



Thermal and mechanical properties of mortars reinforced with recycled brass fibres



R. Borinaga-Treviño ^{a,*}, A. Orbe ^{a,1}, J. Canales ^{a,1}, J. Norambuena-Contreras ^b

^a Department of Mechanical Engineering, University of the Basque Country UPV/EHU, Bilbao, Spain

^b LabMAT, Department of Civil and Environmental Engineering, University of Bío-Bío, Concepción, Chile

HIGHLIGHTS

- Recycled brass fibres from electrical discharge machining were used in mortars.
- 10 mm long fibres did not alter mortar consistency, but 15 mm and 25 mm decreased it significantly.
- Longer fibres and higher fibre proportions increased the thermal conductivity of the mortars.
- Mechanical properties were significantly improved with 15 mm and 25 mm long fibres.

ARTICLE INFO

Article history:

Received 11 June 2020

Received in revised form 15 February 2021

Accepted 23 February 2021

Available online 10 March 2021

Keywords:

Cement mortars

Brass fibres

Electrical discharge machining

Ultrasonic time

Waste

Thermal conductivity

ABSTRACT

This paper aims to encourage the circular economy and merge the manufacturing and the construction industries, providing waste fibres from the electrical discharge machining of the former as raw material for the latter. The research analyses the effect on the physical, thermal and mechanical properties of mortars reinforced with brass fibres. The manuscript deals with different fibre length (10 mm, 15 mm and 25 mm) in variable percentages (0.5%, 1%, 2% and 4%). Larger amounts and longer fibres tend to increase the thermal conductivity whereas post cracking flexural strength is more dependent on fibre length.

© 2021 The Authors. Published by Elsevier Ltd. This is an open access article under the CC BY-NC-ND license (<http://creativecommons.org/licenses/by-nc-nd/4.0/>).

1. Introduction

The increment in the consumption of raw materials in the industry, primarily, and in the construction sector specially, has created a growing awareness of sustainability issues. Among those materials, concrete and mortars stand out as the most widely used construction materials. Within this framework, several are the attempts to reduce the carbon footprint of the fabrication of cementitious materials. Auspiciously, cement-based matrices are very suitable to accept different kinds of by-products as substitute of raw aggregates or reinforcement, maintaining or even improving its physical and mechanical properties. There are several works on this topic [1–7], where industrial waste (e.g. crushed particles or

fibres, polymer powder, solid construction waste, etc.) has replaced the cement, the fine aggregates, or the coarse aggregates within the mixture of the cementitious matrix or its reinforcement.

In this context, end-of-life tyres are an increasing threat to the environment due to the huge disposed amounts. Studies have assessed the durability [1] or the damping properties increment for railway sleepers with rubber additions, satisfying the required concrete strength [2]. Overall, the addition of sawdust improves the thermal behaviour of concrete masonry units, while the lime mud disposed from the paper mill industry prevents a strength reduction due to the timber waste [3]. Electric arc furnace slag is also an adequate substitute of the aggregates in inland and inshore environments as denoted by satisfactory durability tests [4]. Some researches analyse coral waste to mix an adequate concrete for marine environments [5], improving its behaviour up to a certain amount of waste. Other study cases also endorse the feasibility on the use of construction and demolition waste (CDW) within the construction sector overall and the concrete mixing in particular [6], and although current regulations promote the valorisation

* Corresponding author.

E-mail address: roque.borinaga@ehu.eus (R. Borinaga-Treviño).

¹ Permanent address: Department of Mechanical Engineering, University of the Basque Country, Escuela de Ingeniería de Bilbao, Plaza Torres Quevedo, 1, 48013 Bilbao, Bizkaia, Spain.

of the CDW, the recovery target established for 2020 is not currently fulfilled [7].

In accordance to the topic covered by this research, also multiple industries has valorised their fibre type by-products to cover the needs of the construction sector. A comprehensive review of almost 200 research [8] has identified plastic (mainly bottles but also textile, bags and more) and metal fibres (mainly from tyres, but also other industrial by-products) as the most used waste materials for reinforcing cementitious matrices. Nonetheless, there is plenty of literature regarding natural fibres [9]. Since the interest in recycled fibres is increasing exponentially, several research lines in this field are branching out. Besides the initial aim of improving the strength and ductility of the initially brittle cementitious matrix [10,11], the scope is widening to cover cement mortars for self-monitoring purposes with a remarkable reduction in its electrical resistivity [12], above even an order of magnitude [13]. Thus, the environmental benefits may also lead to cost-benefit savings of a 400% [14].

Previous studies have also analysed the mechanical behaviour of concrete reinforced with machining metal discards [15–17]. These discards are cut in up to 50 mm long fibres, presenting a rectangular cross-section. The variability in their mechanical properties and their irregularity, proves inefficient as concrete reinforcement material [15]. Other studies denoted an increment in mechanical properties of the concrete when adding metal drilling waste, in a similar way that raw fibres do. Besides, when combined with silica fume, the improvement is positively increased [16]. Brass fibres have also been previously added to concrete. Although an increment in mechanical properties is reported, the origin and characteristic of those fibres is not accurately described [17].

This research focuses on the brass fibres obtained from Electrical Discharge Machining (EDM) manufacturing process. EDM is a widely used manufacturing process that covers a 7% of the market penetration among the manufacturing methods [18], which comprises the 37% of worldwide energy consumption [19]. Since EDM is known as one of the least environmentally friendly techniques, recent research is focused on optimising such process regarding energy, emissions and other hazards [20]. Besides some other negative environmental impacts, EDM produces a residue as short brass fibres. These fibres derive from the wire used as the tool electrode during the cutting process. Although previous studies represent an advance from an environmental point of view, none of them considers including the generated brass waste as a topic to improve the global performance of the process.

Although brass fibres can easily be recast with the aim of reusing them for any new purpose, this entails a large energy expenditure to which the corresponding impact in terms of emissions and consumption of fossil fuels due to transport must be added. This paper aims of encouraging the circular economy, and merges both industries, namely the manufacturing and the construction sectors, providing waste material of the former as raw material for the latter, without increasing its embodied energy. Therefore, reusing the fibres as mortar reinforcement, may lead to avoid such environmental impact involved, while reducing also that related to the production of raw reinforcement. The present study analyses the fresh and hardened, physical and mechanical properties of several mortars mixed with the addition of raw and reused brass fibres in

different lengths and amounts. Moreover, it focuses in the thermal behaviour of such composite material, providing adequate application recommendations.

2. Materials and methods

2.1. Raw materials

All the mortars were mixed with the same components: water (w), cement (c), superplasticizer (sp), limestone sand (s) and a variable type and proportion of brass fibre. CEM II-B (L)/32.5R type cement was used in agreement with EN 197–1. This Portland cement contains up to 35% of limestone filler by weight, and is adequate for its use in foundation concretes and masonry mortars in general. According to the manufacturer, its compressive strength is higher than 13.5 MPa and 42.5 MPa at an age of 2 days and 28 days, respectively. In addition, 1% by unit weight of cement of BASF-Masterease5038 superplasticizer was also added for obtaining a nearly self-consolidating, non-reinforced, reference mortar. Properties of the limestone sand used in this study are summarised in Table 1. Grain size distribution, apparent particle density (ρ_1) and water absorption were obtained based on their corresponding European Norms (EN 933–1; EN 1097–6).

The difference between the mortars lies on the fibre type, proportion and length used. Both fibre types were obtained by cutting the brass wire used for the electrical discharge machining process. To obtain raw, not-machined (NM) fibres, electrical discharge machine was only used to cut the brass wire, but no electrical discharge machining was applied, so brass remained unaltered after all the process. However, for the recycled, machined fibres (M), fibres were obtained during the usual operation of the electrical discharge machining equipment; hence, fibres were machined before the final cutting process. Although influence of the machining process on the properties of the fibres was already addressed in a previous publication [21], Fig. 1 shows the surface rugosity of both fibre types on the longitudinal direction, measured with Leica DCM3D optical microscope. Due to the machining process, M fibres had a 400% rougher surface than NM fibres, which could lead to differences in their behaviour as reinforcement material. Four different fibre proportions were studied, 0.5%, 1%, 2% and 4% by unit volume of mortar, covering most of the fibre proportions normally used in fibre reinforced mortars and concretes.

Three different fibre lengths were used, 10 mm, 15 mm, and 25 mm. The electrical discharge machining equipment has an integrated cutting system that changes the cutting frequency as a function of the wire longitudinal speed used on the machining process. As a result, fibres always had almost the same length, 8–11 mm [21]. Thus, to obtain the required lengths, the internal cutting system was disconnected and replaced by the external cutting system shown in Fig. 2. It consists on a monophasic electrical engine, a variable intensity and voltage power supply, a rotating disc and a pair of cutting blades. Given the wire longitudinal speed of the equipment, the required fibre lengths were easily obtained by varying the rotational speed of the electrical motor. Fig. 3 shows the final appearance of the six fibre type and length combinations used in this case.

Table 1
Grain-size distribution of the limestone aggregate.

Sieve size [mm]	4	2	1.18	0.6	0.4	0.2	0.1	0.063
% Pass	100	92	68	44	35	22	15	13
Particle apparent density [kg/m ³]	2758							
Water absorption [%wt]	0.45							

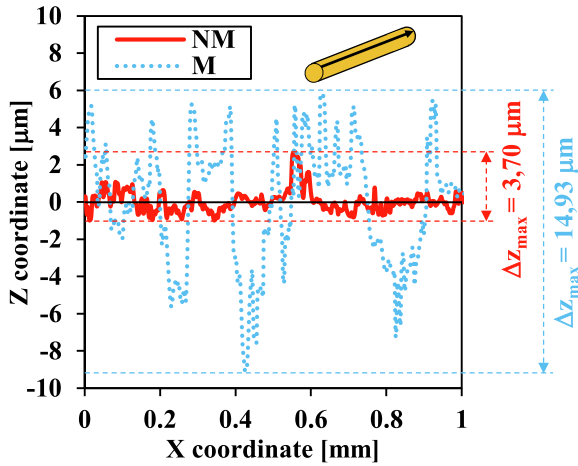


Fig. 1. Rugosity of machined (M) and not machined (NM) fibres, longitudinal direction.

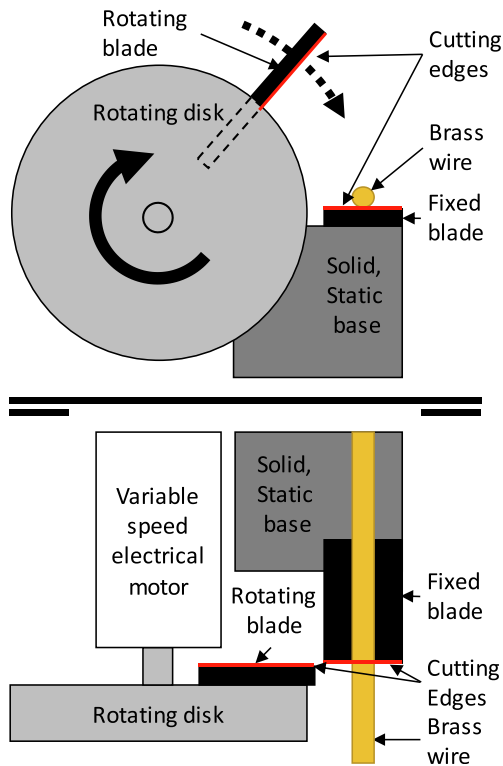


Fig. 2. Sketch of the wire cutting system appended to the existing Electrical Discharge Machining equipment.

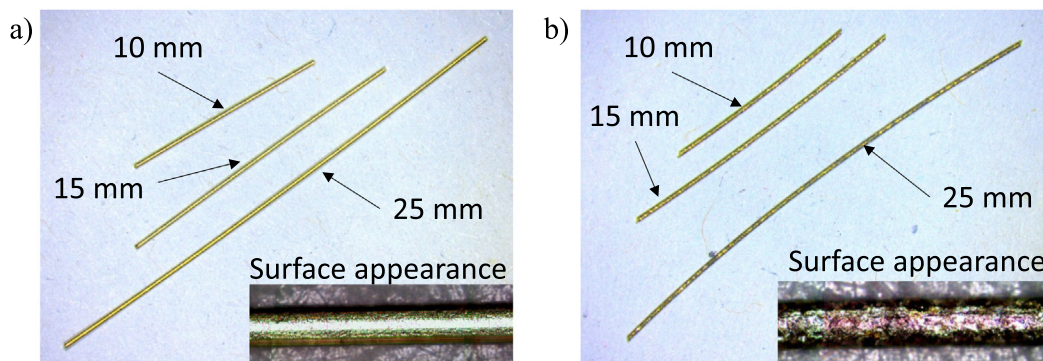


Fig. 3. Fibres used in this experiment: a) Not-machined fibres; b) Machined fibres.

2.2. Mix proportions of the cement mortars

Table 2 shows the proportions for all the cement mortars mixed in this study. A self-compacting mortar without any fibre addition was used as a reference and compared to the other mixes in terms of fresh and hardened properties. All the mortars had the same water:cement:limestone-sand:superplasticizer proportions by weight, 0.65:1:3:0.01. Thus, they only differed on the fibre type, length and proportion used in the mix. For each mortar, three $40 \times 40 \times 160 \text{ mm}^3$ prismatic test specimens were prepared according to EN 1015–10. Mixing process was divided in two different phases. The first phase consisted on mixing the reference mortar that was common in all the studied mixes. Initially, cement and limestone sand were dry-mixed for one minute at low speed. Then, half of the water required by the mix was added and mixed for another minute at the same speed. Immediately after, the rest of the water and the superplasticizer were added and mixed in similar conditions for another minute. Finally, mortar was mixed for another minute at high speed, mixing process was interrupted for two minutes, and mixed it again for another minute at high speed to finish the mixing process of the basic mortar.

For the other mortars, fibres were gradually added to the basic mortar with the mixer working at low speed and finally mixed at low speed for at least another minute. To avoid clogging the mixer during this process, the mixing for higher fibre proportions took longer time in this second phase, for a maximum of three minutes for the highest length and proportion combination studied. After finishing the mixing process, fresh mortar was poured to the centre of each prismatic mould to provide a more homogeneous fibre distribution inside the specimens. Due to the low workability of some of the mortars, mixture had to be manually spread by a spatula. Even though the compaction process was not necessary for all the mortars, all the moulds were vibrated at a frequency of 300 Hz for 30 s to compact all the mixes equally. Then, specimens were sealed and kept for two days on laboratory, to be later submerged in water bath at 20 °C for another 28 days, completing the curing age set in this study. Overall, 75 prismatic specimens ($40 \times 40 \times 160 \text{ mm}$) were cast, three for each mix considering fibres of 10 mm, 15 mm and 25 mm-length with different amounts, 0.5%, 1%, 2% and 4%.

2.3. Experimental characterisation of the cement mortars

To determine the potential use of brass fibres as mortar reinforcement, fresh and hardened properties of the mortar were evaluated. On the one hand, fresh consistency of the mortar was measured via flow table consistency test (EN 1015–3). On the other hand, physical, thermal, and mechanical properties of the hardened mortar were also determined after 28 days of curing time. Dry bulk density (ρ) and water accessible porosity (n) were measured on each specimen according to the standard EN 1015–10.

Table 2
Mix proportions used in this study.

Mix ID [Fibre type-%-length]	Cement [g]	Limestone Sand [g]	Water [g]	Super-Plasticizer [g]	Fibre Length [mm]	Fibre [g]
<i>Reference mortar, without fibres</i>						
Reference	500	1500	325	5	–	0
<i>Raw, not machined fibres (NM)</i>						
NM-0.5%-10 mm	500	1500	325	5	10	42
NM-1%-10 mm						85
NM-2%-10 mm						170
NM-4%-10 mm						340
NM-0.5%-15 mm	500	1500	325	5	15	42
NM-1%-15 mm						85
NM-2%-15 mm						170
NM-4%-15 mm						340
NM-0.5%-25 mm	500	1500	325	5	25	42
NM-1%-25 mm						85
NM-2%-25 mm						170
NM-4%-25 mm						340
<i>Recycled, machined fibres (M)</i>						
M-0.5%-10 mm	500	1500	325	5	10	42
M-1%-10 mm						85
M-2%-10 mm						170
M-4%-10 mm						340
M-0.5%-15 mm	500	1500	325	5	15	42
M-1%-15 mm						85
M-2%-15 mm						170
M-4%-15 mm						340
M-0.5%-25 mm	500	1500	325	5	25	42
M-1%-25 mm						85
M-2%-25 mm						170
M-4%-25 mm						340

Furthermore, Ultrasonic Pulse Velocity (UPV) was measured on the longitudinal direction of the specimens by using a Proceq Pundit PL200 ultrasonic velocity tester to detect possible gaps on the specimens that could indicate an insufficient compaction energy. To guarantee a good contact of the 150 kHz piezoelectric transmitters with the tested specimens, petroleum jelly was used on all the tests. After UPV tests, flexural strength was determined based on EN 1015–11 standard. Flexural test was displacement-controlled (speed ratio 0.5 mm/min) to additionally evaluate the post-cracking behaviour of the fibre-reinforced mortars. With the resulting halves from Flexural test, thermal conductivity (λ) and thermal diffusivity (α) were obtained with a HotDisk M1 tester, which is based on the Transient Plane Source (TPS) method developed by Gustafsson [22]. Test procedure is already explained and used in previous studies [21,23].

In a subsequent stage, compressive strength was determined in agreement with the EN 1015-11 standard, with a load increment ratio of 0.5 kN/s. Representative values of density, porosity, UPV, thermal conductivity, volumetric heat capacity and flexural strength were obtained as the mean of the results obtained on three specimens per mortar studied. However, for the compressive strength, the representative value was obtained as the mean of the results on the six halves available.

To finish with the characterization of the mortar, X-ray computed tomography (CT scan) was employed to evaluate the porosity and fibre distribution of the hardened mortar. With that in mind, a half of each mortar was used ($40 \times 40 \times 80 \text{ mm}^3$), see Fig. 4. The X-ray tomography scans were carried out using GE SEIFERT X-CUBE Compact machine operated at 145–195 kV and 4–10 mA. The software used for 3D volume and 2D image processing was VGStudio MAX version 2.2

3. Results and discussion

3.1. Consistency of the fresh cement mortar

The influence on the fresh consistency of the mortar induced by different fibre types, lengths and proportions was analysed. As

shown in Fig. 4, there is a uniform distribution of fibres and pores, without any significant fibre clusters that would denote problems during the mixing process. It was observed (see Fig. 5) that the fibre type, proportion and length had a significant effect on the fresh consistency of the mortar, except for the NM-10 mm mortars, where the differences are negligible (all the consistencies had a maximum standard deviation of 7 mm, less than that allowed by EN1015-3 standard). NM-10 mm fibres did not reduce the consistency of the resulting mortars, as their smooth surface and reduced length enabled a nearly non-friction sliding between them. Apart from that, it is evident that in spite of the considered fibre length, the higher the fibre proportion used, the lower it was the resulting flow diameter, denoting a significant loss of workability of the mixes. At the same time, when comparing curves for each fibre type, it is also remarkable that, the longer the fibre used, the higher it was the reduction of the flow diameter. Thus, it was challenging to mix NM-2%-15 mm, M-2%-15 mm, NM-4%-15 mm, M-4%-15 mm, NM-2%-25 mm and M-2%-25 mm mortars without clogging the mixer, even impossible for the highest lengths and proportions (NM-4%-25 mm and M-4%-25 mm).

As can be observed in Fig. 5, this trend is valid for both fibre types. Nevertheless, for the same fibre length, the reduction of the flow diameter was more pronounced on mortars reinforced with recycled, machined fibres, which is attributed to the higher surface roughness of the machined fibres.

3.2. Density and porosity of the hardened cement mortars

Fig. 6 shows the density and porosity results of the evaluated mortars. Results indicate that, for each fibre type, the higher the fibre amount used as a reinforcement, the higher it was the density of the resulting mortar. The expected density of the resulting mortar is shown with a red line in Fig. 6, in case the mortar matrix maintained a constant porosity in all the mixes. It is clear that regardless the fibre type and length studied, density increase was linear and similar, denoting that the water accessible porosity did not differ significantly due to the fibre addition. Therefore, compaction process used evened the mortars in terms of porosity.

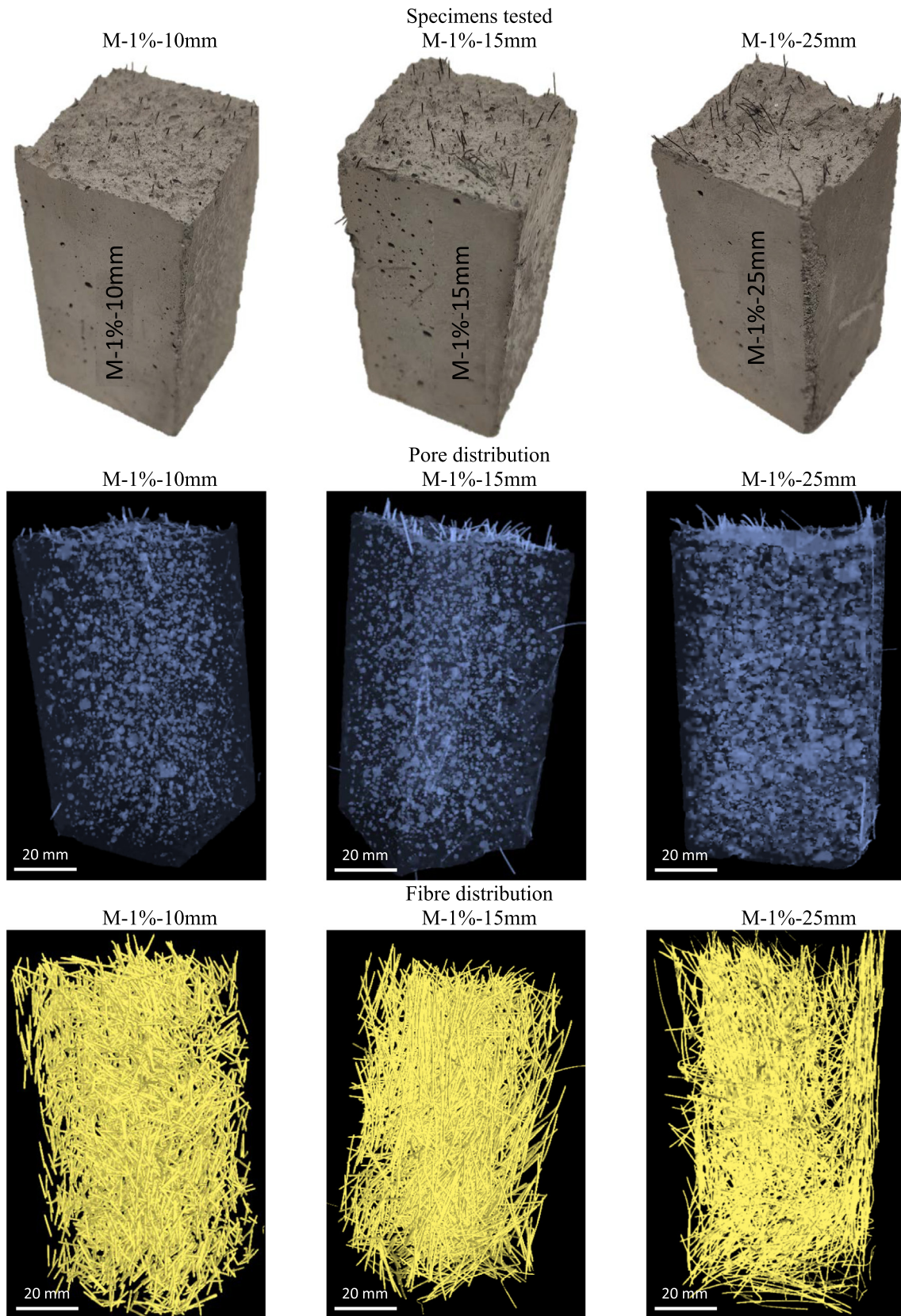


Fig. 4. Specimens subjected to Computed Tomography tests: specimens tested, porosity distribution and fibre distribution.

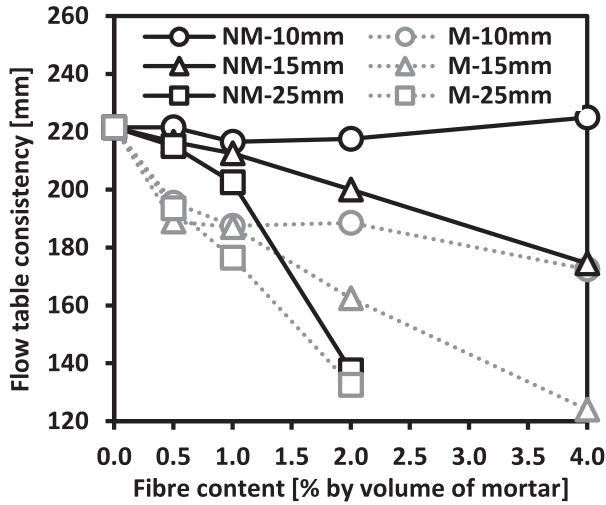


Fig. 5. Consistency results of the fresh mortars on flow table test.

Porosity measurements confirm the previous statement, since slight variations (below 3%) were only detected.

3.3. Ultrasonic pulse velocity of the hardened cement mortars

Fig. 7a shows the Ultrasonic Pulse Velocity results obtained as a function of the fibre type, proportion and length used. In general, the

higher the fibre proportion used, the lower it was the Ultrasonic Pulse Velocity of the resulting mortar. For the mortars reinforced with recycled, machined fibres, UPV was reduced by up to 3% for M-2%-15 mm, M-4%-15 mm and M-2%-25 mm. However, the reduction was more pronounced for the raw fibres, diminishing up to 5.4% and 3.8% for M-4%-10 mm and M-4%-15 mm, respectively.

Initially, this is in contradiction with the water accessible porosity values obtained, as a diminution of the porosity should imply an increase of the UPV. According to the consulted literature, it is not clear the influence of metallic fibre proportion on the UPV of the resulting cementitious composites. Some Authors [17,24] point that UPV increases with the fibre proportion, while other publications indicate the opposite [25–27]. Thus, a statistical study was performed to check if the differences observed with respect to the reference, non-reinforced mortar were significant. For that purpose, normal distribution was used assuming that the differences observed for the different mortars were mainly related to experimental errors. Fig. 7b shows the probability-probability plot adjusted to a normal distribution. Results show a good correlation ($R^2 = 0.9983$) with its corresponding normal distribution, thus the differences observed between the mortars in terms of UPV were not considered statistically significant, as was previously concluded by Yap et al. [28].

As the UPV of brass is higher than the UPV observed on mortars, something is compensating the UPV increase that brass fibres should be giving to the resulting mortar, which is attributed to the higher porosity caused by the fibres. As shown in Fig. 8, water accessible porosity only takes into account the pores that are sub-

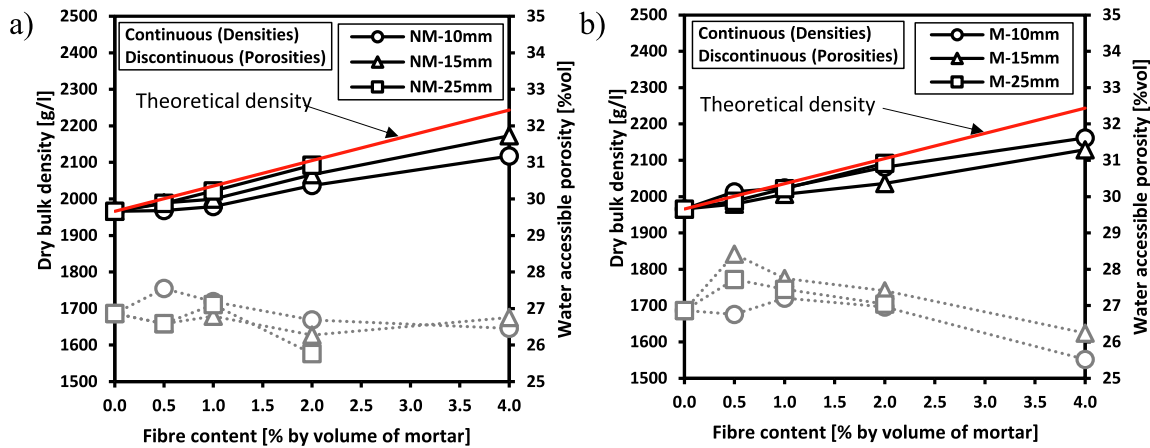


Fig. 6. Influence of the brass fibre type, proportion and length used on dry bulk density and porosity of the hardened mortars: a) Not-machined, raw fibres; b) Machined, recycled fibres.

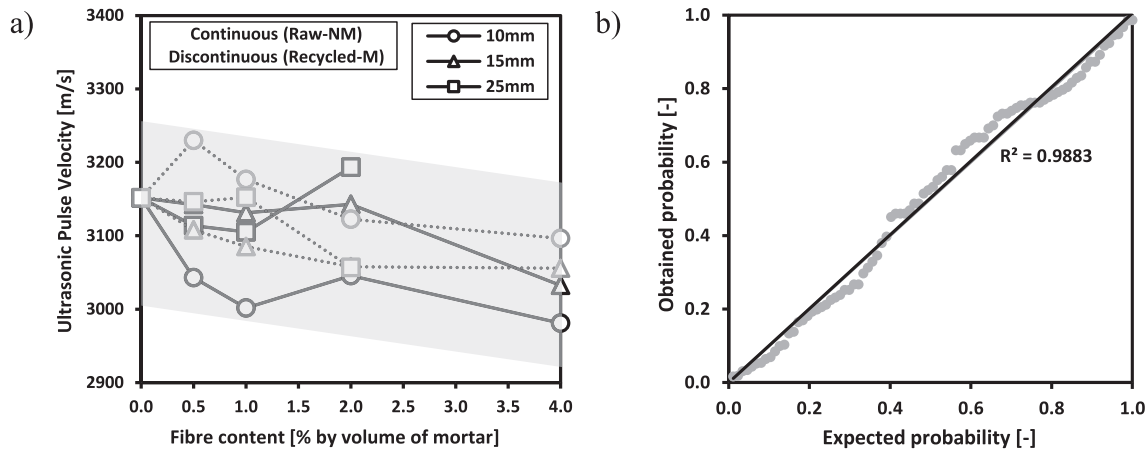


Fig. 7. Influence of the fibre type, proportion and length used on Ultrasonic Pulse Velocity of the mortars: a) Results obtained; b) Normal P-P Plot.

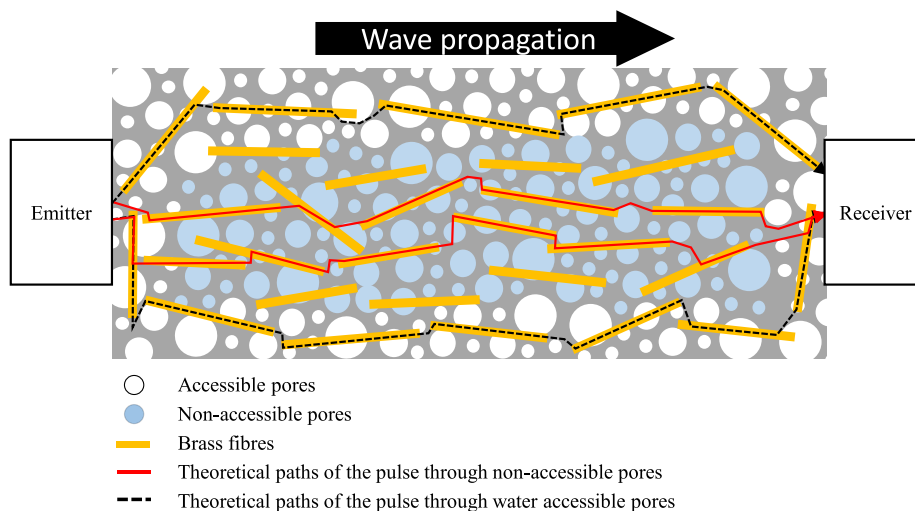


Fig. 8. Possible paths of the pulse through water-accessible or non-accessible pores.

sequently interconnected up to the specimen surface, while the UPV gives an idea of the total porosity. If the material had no pores inside, the path followed by the pulse would always be the same, straight line, which is the distance between the emitter and the receiver, 0.16 m. However, due to the existence of pores and not-completely longitudinally oriented fibres, the real path will be longer than the real distance. Since pores accessible to water are filled with air and non-accessible pores could be partially filled with water, UPV should be faster for the latter. If the fastest path were any path going through the more superficial pores, that is, those that are measured by the water accessible porosity (see Fig. 8, discontinuous paths), UPV results would increase with the fibre content as water accessible porosity values were practically the same for all the mortars. Hence, fibres must be increasing the non-accessible to water porosity in order to maintain similar UPV values. This hypothesis is in agreement with the porosity increase observed on CT-Scan tests. As can be seen in Fig. 4, porosity increased with the fibre length used and similar behaviour is also expected when increasing fibre proportion.

3.4. Thermal conductivity and volumetric heat capacity of the hardened cement mortars

Two variables should be taken into account to determine the influence of the length of the fibres: fibre quantity and fibre-to-fibre interconnection. On the one hand, the shorter the fibre, the higher would be the fibre quantity used for the same proportion, which would increase the probability of having fibre-to-fibre contacts on the mortar. That would enable a more continuous fibre net along the specimen, which would increase the mortar thermal conductivity. On the other hand, each fibre would also be a preferential heating path, thus the longer the fibre, the further would reach the heat once one side of the fibre is heated.

Thermal conductivity of the mortars is shown in Fig. 9a. As expected, a higher fibre proportion implied a higher thermal conductivity of the resulting mortars, due to the higher thermal conductivity of the brass fibres. With the exception of the NM-10 mm mortars, the thermal conductivity increased linearly with the fibre proportion used, denoting that the fibre dispersion and compaction was uniform in all the mixes. NM-4%-10 mm, NM-4%-15 mm and NM-2%-25 mm mortars had a thermal conductivity increment of 53% (standard deviation SD = 9.5%), 44% (SD = 6.4%)

and 40% (SD = 1.4%), with respect to that of the reference mortar, respectively. Similarly, M-4%-10 mm, M-4%-15 mm and M-2%-25 mm mortars increased the thermal conductivity by 49.5% (SD = 2.2%), 49.2% (SD = 1.8%) and 49.2% (SD = 2.3%), respectively, similar to those observed for the raw, not-machined fibres. Please note that the maximum growths were obtained with the highest proportions used in each case, but those proportions were not the same for all the fibre lengths, as the mortars with 4% of 25 mm long fibres were impossible to mix. Therefore, the longest fibres gave similar thermal conductivity increase, but with half of the fibre proportion required by the shorter ones.

Moreover, the higher the fibre length used, the higher was the thermal conductivity increase for the same fibre proportion. As each fibre type had the same diameter for the different lengths studied, the difference in the number of fibres per unit volume of mortar will be inversely proportional to the ratio between the fibre lengths. For instance, there will be 10/25 times less fibres for the 25 mm length than for the 10 mm length. Thus, heat will also require to go through less interconnections for a given mortar thickness, further improving the thermal conductivity of the resulting mortar. At the same time, the increases were also slightly higher on the mortars with recycled fibres than on the mortars with raw fibres. Due to the higher rugosity of the M fibres, there is a higher probability of having multiple contact points on the fibre-to-fibre contact surface, which would reduce its thermal contact resistance (see Fig. 10).

On the other hand, Fig. 9b shows the volumetric heat capacity of the mortars as a function of the fibre type, proportion and length used. In contrast to the behaviour observed for the thermal conductivity, the higher it was the fibre proportion used, the lower it was the volumetric heat capacity of the resulting mortar. As for the thermal conductivity, there is a linear correlation between both parameters. NM-4%-10 mm, NM-4%-15 mm and NM-2%-25 mm mortars had a volumetric heat capacity decrease of 32% (SD = 7.4%), 29% (SD = 0.6%) and 22% (SD = 6.2%), with respect to that of the reference mortar, respectively. In the same way, M-4%-10 mm, M-4%-15 mm and M-2%-25 mm mortars increased the thermal conductivity by 31% (SD = 6.6%), 33% (SD = 8.2%) and 19% (SD = 5.3%), respectively, similar to those observed for the raw, not-machined fibres. Therefore, both fibre types had a similar influence on the volumetric heat capacity of the mortar, with an unclear influence of the fibre length.

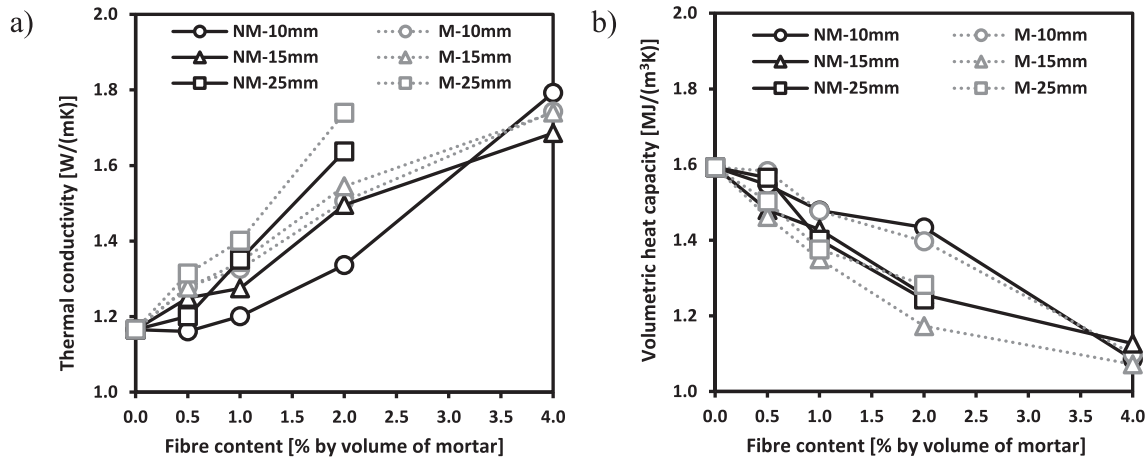


Fig. 9. Influence of the fibre type, proportion and length used on the thermal properties of the mortars: a) Thermal conductivity; b) Volumetric heat capacity.

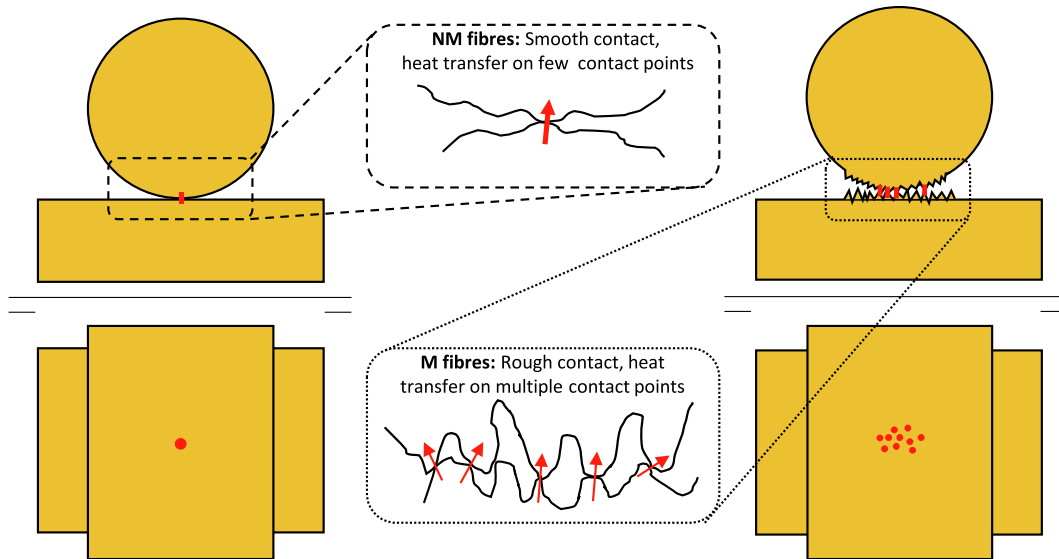


Fig. 10. Smooth contact between NM fibres vs. rough contact between M fibres.

3.5. Mechanical properties of the hardened mortars

Fig. 11 shows the maximum flexural and compressive strengths of the mortar specimens as a function of the fibre type, proportion and length used as reinforcement. For both mortars, regardless the fibre type used, both compressive and flexural strengths increased due to the fibre addition.

In terms of flexural peak strength, mortars presented a higher dependency on the fibre length than on the fibre type used. Overall, the behaviour of both fibre types was quite similar for the same proportions and lengths used. However, flexural peak strength tended to be slightly higher on mortars with the recycled, machined fibres with respect to the values observed on raw, not-machined mortars, which is also attributed to the better anchorage provided by the higher roughness of the recycled fibres. This effect, however, is not very remarkable, since the debonding process had not been fully initialized and the friction on the interface did not contribute substantially. However, fibre length had a notable influence on the mortar flexural peak strength. The longer the fibres used, the higher it was the flexural peak strength of the mortar.

Overall, all the lengths increased the flexural strength of the mortar. NM-4%-10 mm, NM-2%-15 mm and NM-2%-25 mm mor-

tars had a flexural strength gain of 48% (SD = 12.5%), 103% (SD = 18.5%) and 153% (SD = 4.4%), with respect to the reference mortar, respectively; M-4%-10 mm, M-4%-15 mm and M-2%-25 mm mortars increased the flexural strength by 30% (SD = 9.8%), 135% (SD = 11.2) and 154% (SD = 33.8%), respectively. However, not all the fibre lengths increased the flexural strength for lower fibre proportions. While 15 mm and 25 mm long fibres improved the flexural strength in all percentages, 10 mm long fibres required a minimum of 2% to notice a slight improvement, as it was already proved previously [21]. According to Bentur [29], there is a critical length that makes the fibre fail by yield strength instead of being pulled out of the mortar matrix. Above this length, fibre would not provide a higher reinforcing effect to the resulting mortar and its contribution would be ruled by the yield stress of the fibre. However, shorter fibres would provide a reinforcing effect that would be related to its length, but, again, a minimum length would be necessary to provide any reinforcing effect at all. When comparing 10 mm fibres to 15 mm and 25 mm fibres in terms of flexural strength and residual load, it is clear that this secondary minimum length is somewhere between 10 mm and 15 mm, as the former had no reinforcing effect on the resulting mortars. This is in agreement with the results

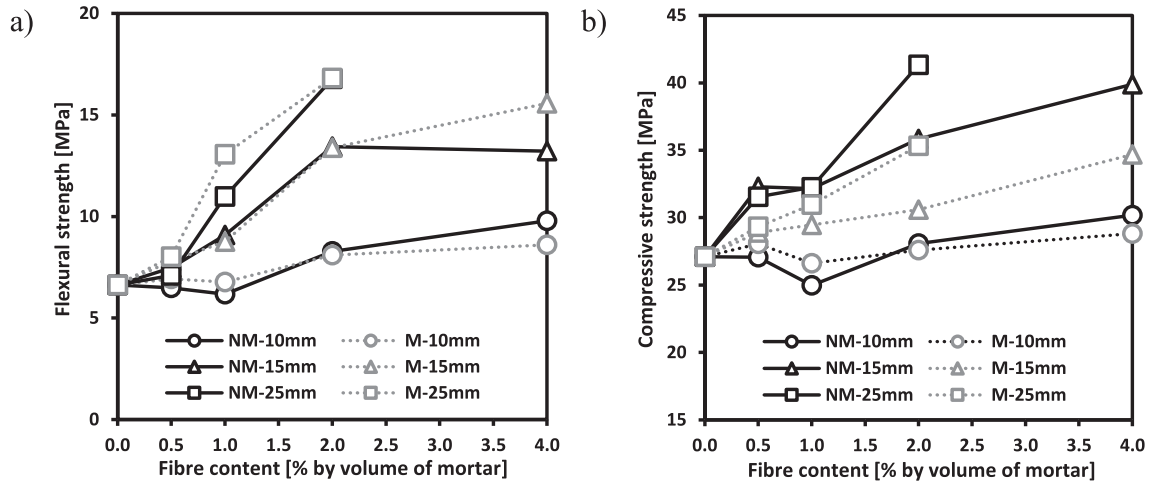


Fig. 11. Influence of the fibre type, proportion and length used on the mechanical properties of the mortars: a) Flexural strength; b) Compressive strength.

obtained by Shannag et al. [30], with the lengths studied by other authors [29,31–33] and with the lengths of commercially available steel fibres used to reinforce mortars. When comparing 15 mm and 25 mm fibres, it is clear that the maximum flexural load is higher

for the mortars with 25 mm fibres. Being 25 mm fibres longer than 15 mm fibres, the critical length of the fibres will be higher than 15 mm as the maximum flexural load of the former was higher than that of the latter.

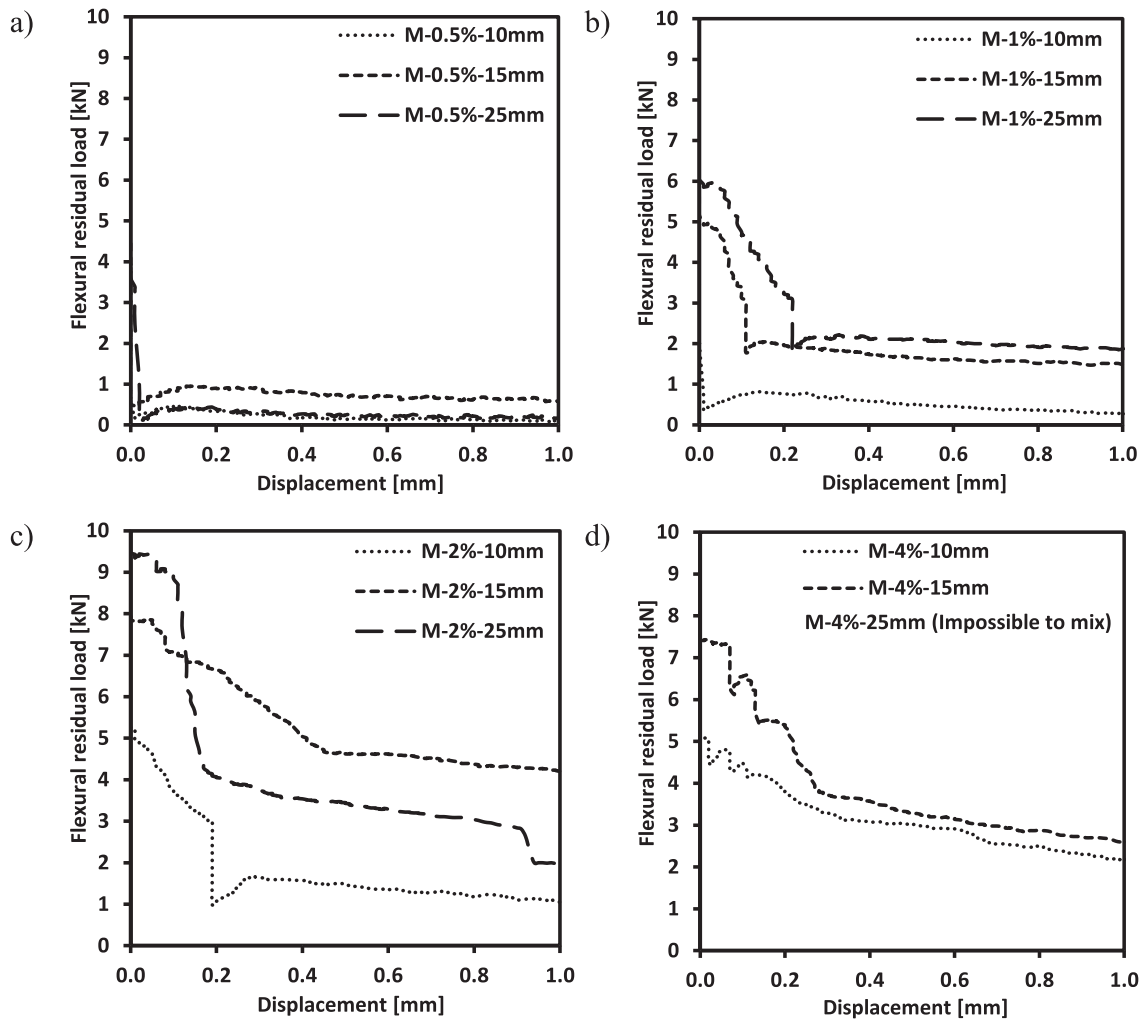


Fig. 12. Influence of the fibre proportion and length used on the post-cracking behaviour of the mortars observed on flexural strength test: a) 0.5%; b) 1%; c) 2%; d) 4%.

Besides, Fig. 12 shows the residual strength curves obtained on flexural tests for all the recycled brass fibre reinforce mortars. The curves represented are the weakest cases observed on each mortar studied. The maximum load achieved corresponds to the initiation of the debonding process of the fibres, which is mainly related to the fibre length [30]. Once this threshold is exceeded, the bearing load drops until the total debonding occurs and the pure friction stage starts [34]. Since for low fibre amounts the matrix is negligibly confined by the fibres, the spalling process, coupled with the debonding process, takes place mainly for the highest fibre percentages, shown as load drops in the descending branch. The number and amplitude of such drops is linked with the fibre orientation. Inclined fibres tend to increase post cracking behaviour [35] and it is obvious that in case of high amount of fibres they tend to hinder each other for aligning horizontally. As illustrated in Fig. 4, due to wall effects in such a reduced size specimen fibres tended to align longitudinally, in accordance with the main tensile stress. This effect was more pronounced for the longest fibres, as the boundary conditions restricted more their final position. However, another key factor is the embedded length and the frictional stage is conditioned by the area of fibre-matrix interface.

On the one hand, it is evident that a minimum of 1% of fibres was necessary to notice a significant post-fracture behaviour, in accordance with the flexural peak strength increment noticed for each percentage. As expected, the higher the fibre content, the higher and the more maintained it was the residual strength of the mortars. However, the increase was not equal for all the fibre lengths. On the other hand, 10 mm long fibres only presented an appreciable residual strength for the highest proportions, as only M-4%-10 mm and NM-4%-10 mm mortars lost progressively their residual strength without any sudden drop. Conversely, mortars with 15 mm long fibres showed overall a better post-fracture behaviour for all the studied proportions. As for the 10 mm long fibres, the higher it was the fibre proportion used, the higher it was also its residual strength, but this increase was optimal for the mortars containing 2% of fibres.

As a result, 25 mm long fibres were the fibres that improved the most the post-fracture behaviour of the resulting mortars, as they experienced less sudden drops of the residual strength, even the residual strength of the M-2%-25 mm and NM-2%-25 mm were comparable to that of the other mortars with 4% of shorter fibres.

To conclude, contribution of the fibres to the compressive strength (see Fig. 11b) differed with respect to that observed for the flexural strength. For the shortest fibre length, contribution was not significant even for the highest fibre proportions, and there was not any difference between the fibre types used. For the lowest proportions (0.5% and 1%), there was even a decrease on the compressive strength. However, 15 mm and 25 mm long fibres did contribute to improve the compressive strength of the mortar, as previous studies confirm [17,35–38]. While NM-4%-15 mm and NM-2%-25 mm mortars increased it by 47% (SD = 5.7%) and 52% (SD = 2.0%), M-M-4%-15 mm and M-2%-25 mm mortars did it by 28% (SD = 2.3%) and 30% (SD = 5.7%). Therefore, raw fibres improved more the compressive strength of the material than recycled fibres, due to the weakening effect caused by the electrical discharge machining process.

4. Conclusions and recommendations

The present study analysed the influence of the length and proportion of waste brass fibres from the electrical discharge machining process on the physical, mechanical and thermal properties of cement mortars. Based on the results, the following conclusions have been obtained:

- The fibre proportion and length influences notably the consistency of fresh mortar. For short fibres and low amounts, the repercussion is negligible, but as long as they increase it becomes hard to mix (15 mm-long fibres) or even an impossible task (25 mm-long fibres). The rugosity observed in the reused fibres led to a larger reduction on the flowability.
- Compaction process overcame the differences observed on flowability. Density increased linearly due to brass fibre addition while water accessible porosity remained similar in all cases.
- Due to the higher non-accessible porosity caused by the fibres, their influence on the ultrasonic pulse velocity of the mortar was not statistically significant.
- In accordance with the aforementioned statements, fibres tended to increase the thermal conductivity and to decrease the volumetric heat capacity of the resulting mortar. The correlation with the fibre proportion was approximately linear, more remarked for the longer fibres and the recycled fibres, for all the fibre type-length combination used.
- With respect to the mechanical properties, both variables were linearly correlated to the fibre proportion used, more noticeably for longer fibres. On the one hand, the increment of the flexural strength was slightly better for recycled fibres while, on the other hand, the compressive strength gain was higher with the raw, not-machined fibres,

Finally, Authors would like to make some recommendations:

- When the flowability of the mortar is crucial (underfloor heating systems, slab repair, etc.), the shortest 10 mm long fibres are recommended, in the highest fibres percentage possible, 2–4%.
- When fresh consistency of the mortar is not an issue, 2% of either 15 mm or 25 mm long fibres are proposed per unit volume of mortar, since they provide the largest improvement on mechanical properties.

CRediT authorship contribution statement

R. Borinaga-Treviño: Conceptualization, Methodology, Investigation, Formal analysis, Writing - original draft. **A. Orbe:** Investigation, Visualization, Writing - review & editing. **J. Canales:** Investigation, Writing - review & editing, Funding acquisition. **J. Norambuena-Contreras:** Methodology, Visualization, Writing - review & editing.

Declaration of Competing Interest

The authors declare that they have no known competing financial interests or personal relationships that could have appeared to influence the work reported in this paper.

Acknowledgements

This work has been partly financed within the European Horizon 2020 Joint Technology Initiative Shift2Rail through contract no. 826255 (IN2TRACK2). This work has also been co-financed with the project Elkartek 2019 ref. KK-2019/00023 (GOLIAT2). The authors also wish to thank the Basque Government for financial assistance through IT919-16 and IT1314-19.

References

- [1] A.A. Ghani, H.H. Alghazali, M.A. ElGawady, J.J. Myers, D. Feys, Durability properties of cleaner cement mortar with by-products of tire recycling, *J. Clean Prod.* 213 (2019) 1135–1146.

- [2] S. Kaewunruen, D. Li, Y. Chen, Z. Xiang, Enhancement of dynamic damping in eco-friendly railway concrete sleepers using waste-tyre crumb rubber, *Mater* (2018) 11.
- [3] M. Madrid, A. Orbe, H. Carré, Y. García, Thermal performance of sawdust and lime-mud concrete masonry units, *Constr. Build. Mater.* 169 (2018) 113–123.
- [4] A. Santamaría, A. Orbe, J.T. San José, J.J. González, A study on the durability of structural concrete incorporating electric steelmaking slags, *Constr. Build. Mater.* 161 (2018) 94–111.
- [5] B. Liu, J. Guo, J. Zhou, X. Wen, Z. Deng, H. Wang, et al., The mechanical properties and microstructure of carbon fibers reinforced coral concrete, *Constr. Build. Mater.* 249 (2020).
- [6] R.V. Silva, J. de Brito, R.K. Dhir, Use of recycled aggregates arising from construction and demolition waste in new construction applications, *J. Clean Prod.* 236 (2019).
- [7] P. Villoria Sáez, M. Osmani, A diagnosis of construction and demolition waste generation and recovery practice in the European Union, *J. Clean Prod.* 241 (2019).
- [8] R. Merli, M. Preziosi, A. Acampora, M.C. Lucchetti, E. Petrucci, Recycled fibers in reinforced concrete: A systematic literature review, *J. Clean Prod.* 248 (2020).
- [9] M.P. Sáez-Pérez, M. Brümmer, J.A. Durán-Suárez, A review of the factors affecting the properties and performance of hemp aggregate concretes, *J. Build. Eng.* 31 (2020).
- [10] E. Martinelli, A. Caggiano, H. Xargay, An experimental study on the post-cracking behaviour of Hybrid Industrial/Recycled Steel Fibre-Reinforced Concrete, *Constr. Build. Mater.* 94 (2015) 290–298.
- [11] J. Norambuena-Contreras, J. Quilodran, I. Gonzalez-Torre, M. Chavez, R. Borinaga-Treviño, Electrical and thermal characterisation of cement-based mortars containing recycled metallic waste, *J. Clean Prod.* 190 (2018) 737–751.
- [12] J. Norambuena-Contreras, A. Cartes, I. Gonzalez-Torre, M. Chavez, A. Kanellopoulos, Effect of metallic waste addition on the physical and mechanical properties of cement-based mortars, *Appl. Sci.* (2018) 8.
- [13] A. Belli, A. Mobili, T. Bellezze, F. Tittarelli, Commercial and recycled carbon/steel fibers for fiber-reinforced cement mortars with high electrical conductivity, *Cem. Concr. Compos.* 109 (2020).
- [14] O. Onuaguluchi, N. Banthia, Scrap tire steel fiber as a substitute for commercial steel fiber in cement mortar: Engineering properties and cost-benefit analyses, *Resour. Conserv. Recycl.* 134 (2018) 248–256.
- [15] F. Grzymiski, M. Musiał, T. Trapko, Mechanical properties of fibre reinforced concrete with recycled fibres, *Constr. Build. Mater.* 198 (2019) 323–331.
- [16] A. Hassani, M. Arjmandi, Enhancement of concrete properties for pavement slabs using waste metal drillings and silica fume, *Waste Manage. Res.* 28 (2010) 56–63.
- [17] R.A. Zubaidi, S. Barakat, S. Altoubat, Effects of adding brass byproduct on the basic properties of concrete, *Constr. Build. Mater.* 38 (2013) 236–241.
- [18] W. Ming, Z. Zhang, S. Wang, Y. Zhang, F. Shen, G. Zhang, Comparative study of energy efficiency and environmental impact in magnetic field assisted and conventional electrical discharge machining, *J. Clean Prod.* 214 (2019) 12–28.
- [19] C. Park, K. Kwon, W. Kim, B. Min, S. Park, I. Sung, et al., Energy consumption reduction technology in manufacturing - A selective review of policies, standards, and research, *Int. J. Precis. Eng. Manuf.* 10 (2009) 151–173.
- [20] J.B. Valaki, P.P. Rathod, B.C. Khatri, Environmental impact, personnel health and operational safety aspects of electric discharge machining: A review, *Proc. Inst. Mech. Eng. Part B J. Eng. Manuf.* 229 (2015) 1481–1491.
- [21] R. Borinaga-Treviño, A. Orbe, J. Canales, J. Norambuena-Contreras, Experimental evaluation of cement mortars with recycled brass fibres from the electrical discharge machining process, *Constr. Build. Mater.* 246 (2020).
- [22] S.E. Gustafsson, Transient plane source techniques for thermal conductivity and thermal diffusivity measurements of solid materials, *Rev. Sci. Instrum.* 62 (1991) 797–804.
- [23] R. Borinaga-Treviño, A. Orbe, J. Norambuena-Contreras, J. Canales, Effect of microwave heating damage on the electrical, thermal and mechanical properties of fibre-reinforced cement mortars, *Constr. Build. Mater.* 186 (2018) 31–41.
- [24] A.S.D. Al-Ridha, A.A. Abbood, S.F. Al-Chalabi, A.M. Aziz, L.S. Dheyab, A comparative study between the effect of steel fiber on ultrasonic pulse velocity (UPV) in light and normal weight self-compacting concretes, *IOP Conf. Ser. Mater. Sci. Eng.* (2020) 888.
- [25] J. Carrillo, J. Ramirez, J. Lizarazo-Marriaga, Modulus of elasticity and Poisson's ratio of fiber-reinforced concrete in Colombia from ultrasonic pulse velocities, *J. Build. Eng.* 23 (2019) 18–26.
- [26] S. Hedjazi, D. Castillo, Relationships among compressive strength and UPV of concrete reinforced with different types of fibers, *Heliyon* (2020) 6.
- [27] S. Mehdi-pour, I.M. Nikbin, S. Dezhampannah, R. Mohebbi, H. Moghadam, S. Charkhtab, et al., Mechanical properties, durability and environmental evaluation of rubberized concrete incorporating steel fiber and metakaolin at elevated temperatures, *J. Clean Prod.* 254 (2020).
- [28] S.P. Yap, U.J. Alengaram, M.Z. Jumaat, The effect of aspect ratio and volume fraction on mechanical properties of steel fibre-reinforced oil palm shell concrete, *J. Civ Eng Manage* 22 (2016) 168–177.
- [29] A. Bentur, S. Mindess, *Fibre reinforced Cementitious Composites*, CRC Press, 2006.
- [30] M.J. Shannag, R. Brincker, W. Hansen, Pullout behavior of steel fibers from cement-based composites, *Cem. Concr. Res.* 27 (1997) 925–936.
- [31] C. Zanotti, G. Rostagno, B. Tingley, Further evidence of interfacial adhesive bond strength enhancement through fiber reinforcement in repairs, *Constr. Build. Mater.* 160 (2018) 775–785.
- [32] E. Choi, D. Joo Kim, H. Youn, T. Nam, Repairing cracks developed in mortar beams reinforced by cold-drawn NiTi or NiTiNb SMA fibers, *Smart Mater. Struct.* (2015) 24.
- [33] S. Aydin, B. Baradan, The effect of fiber properties on high performance alkali-activated slag/silica fume mortars, *Compos. Part B: Eng.* 45 (2013) 63–69.
- [34] F. Laranjeira, A. Aguado, C. Molins, Predicting the pullout response of inclined straight steel fibers, *Mater. Struct.* 43 (2010) 875–895.
- [35] V.M.C.F. Cunha, J.A.O. Barros, J.M. Sena-Cruz, Pullout behavior of steel fibers in self-compacting concrete, *J. Mater. Civ. Eng.* 22 (2010) 1–9.
- [36] P.S. Song, S. Hwang, Mechanical properties of high-strength steel fiber-reinforced concrete, *Constr. Build. Mater.* 18 (2004) 669–673.
- [37] M.C. Nataraja, N. Dhang, A.P. Gupta, Stress-strain curves for steel-fiber reinforced concrete under compression, *Cem. Concr. Compos.* 21 (1999) 383–390.
- [38] J.A. Carneiro, P.R.L. Lima, M.B. Leite, R.D. Toledo Filho, Compressive stress-strain behavior of steel fiber reinforced-recycled aggregate concrete, *Cem. Concr. Compos.* 46 (2014) 65–72.